Environ Sci Pollut Res (2018) 25:20385–20390
DOI 10.1007/s11356-017-9362-1

Detection of typhoid fever by diatom-based optical biosensor

Viji Selvaraj[1] · **Anbazhagi Muthukumar**[2] · **Ponpandian Nagamony**[1] · **Viswanathan Chinnuswamy**[1]

Received: 2 February 2017 / Accepted: 23 May 2017 / Published online: 2 June 2017

Abstract Surface-modified diatom substrates are employed for the development of immunocomplex-based optical biosensor for diagnosis of typhoid. Biosensor has been prepared by covalent immobilization of *Salmonella typhi* antibody onto the crosslinked diatom substrates via glutaraldehyde. Photoluminescent (PL) studies revealed good specificity and ability of conjugated diatom substrates to distinguish complementary (*S. typhi*) and non-complementary (*Escherichia coli*) antigens. The immunocomplexed biosensor showed detection limit of 10 pg. The excellent performance of biosensor is associated to its large surface-to-volume ratio, good photoluminescent property, and biocompatibility of diatom frustules, which enhances the antibody immobilization and facilitates the nucleophilic electron transfer between antibody and conjugated diatom surface. Hence, immunocomplexed diatom substrates are considered to be a suitable platform for the environmental monitoring of water-borne pathogen *S. typhi*.

Keywords Diatom · *S. typhi* · Biosensor · Antibody · Antigen · Environmental monitoring

Responsible editor: Philippe Garrigues

✉ Viswanathan Chinnuswamy
viswanathan@buc.edu.in

[1] Department of Nanoscience and Technology, Bharathiar University, Coimbatore, Tamilnadu 641 046, India

[2] Department of Environmental Sciences, Bharathiar University, Coimbatore, Tamilnadu 641 046, India

Introduction

Water-borne pathogens are identified as major cause of infectious disease in humans worldwide (Pui et al. 2011). Typhoid, cholera, hepatitis, bacillary dysenteries, diphtheria, salmonellosis, listeriosis, pneumonia, meningitis, and several other gastrointestinal diseases are common water-borne diseases. Typhoid, caused by a water-borne intracellular pathogen *Salmonella enteric* serovar *typhi* (*S. typhi*) is considered as a life-threatening illness (Zhang et al. 2008). Typhoid fever occurs in areas having unhygienic potable water with improper sanitation systems (Sharan et al. 2011). The conventional bacterial culture method and Widal test detect the infection at the advanced stages and so its morbidity and mortality rates are very high. The highly sophisticated methods such as immunological detection and molecular techniques are expensive and required trained personnel (Singh et al. 2012). Thus, it is very important to develop a method for early detection of *S. typhi* which enables both clinical diagnostics and environmental monitoring.

The latest progresses in molecular bioelectronics have facilitated the development of highly selective biosensor system (Betard and Fischer 2012). Various biosensing applications of nanomaterials have improved the performance of point-of-care diagnostics in medical field. A variety of nanomaterials such as gold, silver, zinc oxide, carbon nanotubes, graphene, iron oxide, and composites have been reported for their use in the fabrication of biosensors. Among these, a silica-based natural nanoporous material with innate photoluminescent property called diatom is considered to be a promising material for sensing platform. The attachment of desired biomolecules to the diatom surface is facilitated by a variety of functional groups such as OH, COOH, and CHO (Han et al. 2011).

Debra K Gale and co-workers have described a photoluminescent sensor based on antibody-functionalized

diatom biosilica for the detection of goat anti-rabbit IgG molecules (Gale et al. 2009). Amine-functionalized diatom frustules have been utilized for the detection of BSA protein with a detection limit up to 3×10^{-5} M (Viji et al. 2014). The silica skeleton of marine diatoms *Thalassiosira rotula* shows that PL depends strongly on the surrounding environment. Significant variation of PL intensity, even at low (sub-ppm) NO_2 concentrations, has been observed for *T. rotula* frustules, and saturation of the quenching effect occurs at NO_2 concentrations of the order of 10 ppm (Lettieri et al. 2008; De Stefano et al. 2005).

This study is showing application of crosslinked amine-functionalized diatom substrates for the rapid and selective detection of typhoid. The analytical performance of the designed photoluminescent biosensor has been evaluated for the *S. typhi* and *E. coli* antigens using photoluminescent spectroscopy.

Materials and methods

Materials

3-Aminopropyltriethoxysilane (APS) (analytical grade, 98%), glutaraldehyde solution ($C_5H_8O_2$) (25%), and ethanol absolute (C_2H_5OH) (analytical grade, 99.9%) were purchased from HiMedia chemicals. *S. typhi* antibody and antigen are purchased from BeneSphera - Widal test kit from Avantor company. Double distilled water was used for the preparation of all solutions.

Preparation of diatom substrates for sensing experiment

The mass culture of *Amphora* sp. diatoms was obtained from Marine Planktonology & Aquaculture Lab, Department of Marine Science, Bharathidasan University, Tiruchirappalli, Tamilnadu. The obtained diatoms were centrifuged and rinsed with distilled water to remove salt contents. Samples were treated with 50:50 (v/v) water followed by 30% hydrogen peroxide, and incubated at 90 °C for 3–4 h, followed by the addition of hydrochloric acid to remove the organic matter and clean the frustules. Samples were collected by sieving to prevent damage to the frustules, rinsed copiously with distilled water, and stored in 70% ethanol (Yu et al. 2010).

The diatom frustule surface of *Amphora* sp. was chemically modified as follows: a 10 mg of diatom frustules, 10 mL of ethanol, and 3% of APS were mixed together and heated to 65 °C in a shaking incubator for 1 h (De Stefano et al. 2008, 2009). The reactant solution was centrifuged for 10 min at 3000 rpm and washed in ethanol for several times to remove excess APS. The amine-functionalized diatom frustules (AFD) were spin-coated in a clean glass substrate and heated for 1 h in hot air oven at 90 °C. This resulted in uniformly coated AFD substrates.

For crosslinking, an AFD substrate was transferred to a single-well in polystyrene six-well plate containing 1.8 mL of PBS buffer, in which 200 μL of glutaraldehyde was added, and then the suspension was mixed in a shaking incubator at room temperature for 20 min. The crosslinked substrates were washed in PBS buffer for three times to remove excess of crosslinkers.

The covalent immobilization of *S. typhi* antibody was done by placing crosslinked substrates into a six-well plate containing 1.8 mL of PBS buffer, and 200 μL of antibody was added to it. The substrates were mixed in a shaking incubator at room temperature for 2 h. The *S. typhi* antibody-conjugated diatom frustule substrates were rinsed in PBS buffer. All the experiments were done in triplicate.

The *S. typhi* antibody-conjugated diatom frustule substrates were challenged with different concentrations of its *S. typhi* O and H antigens. The stocks of O and H antigens were prepared at 10^{-3} concentration and from that the working solution was prepared by adding 200 μL of antigen to 1.8 mL of PBS buffer. A 200 μL of antigens from the working solution was taken and was serially diluted from 10^{-1} to 10^{-7} and added to the *S. typhi* antibody-conjugated diatom frustule substrates in the presence of PBS buffer, and the substrates were mixed in an incubator shaker at room temperature for 2 h. The *S. typhi* antibody and *S. typhi* antigen formed the immunocomplex by bonding with each other. The immunocomplexed diatom frustule substrates were then rinsed in PBS buffer.

Results and discussion

Morphological analysis

In Fig. 1a, c, field-emission scanning electron microscopic (FESEM) image of AFD and glutaraldehyde-crosslinked AFD was reported. The result clearly indicates that there is a difference in the morphology of AFD and crosslinked AFD. The AFD has a uniform coating of APS over its surface, and there was some gap in the center of pores, whereas in crosslinked AFD, it majorly covers the whole structure and has a smooth outer structure. It is because of the amine functionalization made the diatom surface more reactive and formed large complex between the long-chain structure of glutaraldehyde and the free amine group of AFD (Li et al. 2013). The presence of elements was confirmed using energy dispersive spectroscopic (EDS) spectrum (Fig. 1b, d).

Functional group analysis

The infrared spectra of AFD and crosslinked AFD were shown in Fig. 2. The vibrations in the range of 541, 599, and 637 cm^{-1} were observed with increased intensities

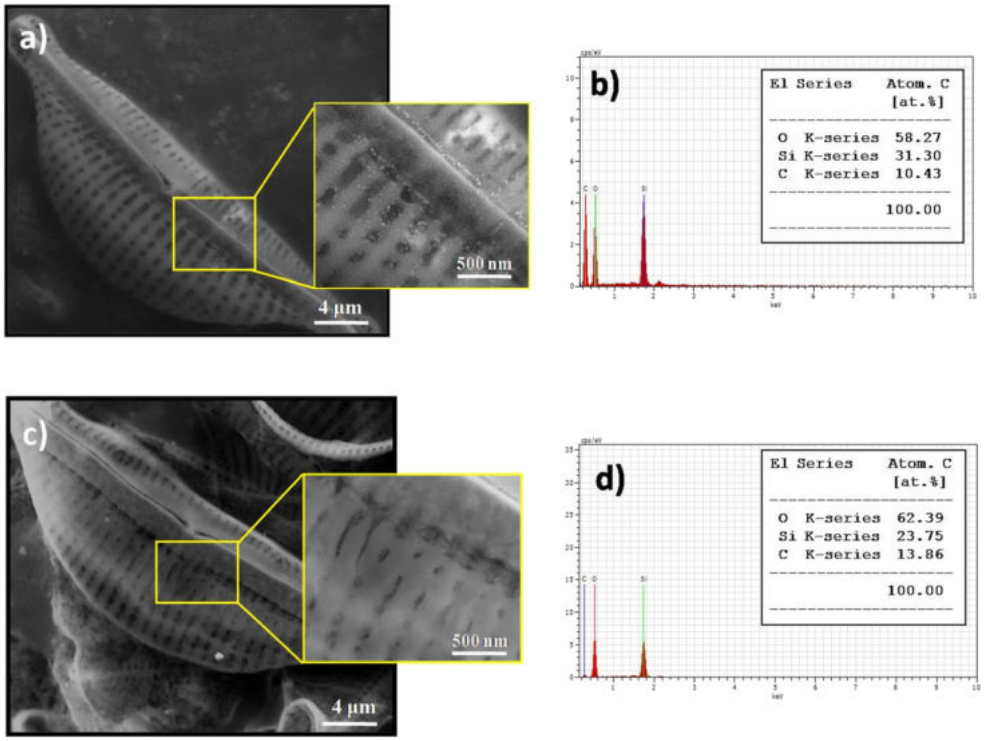

Fig. 1 (**a**) Electron microscopic image (*inset*: higher magnification image) and (**b**) EDS spectrum with chemical composition of AFD; (**c**) electron microscopic image (*inset*: higher magnification image) and (**d**) EDS spectrum with chemical composition of crosslinked AFD substrate

compared to that of AFD. The characteristic peaks observed from 1087 to 1667 cm^{-1} in the AFD were shifted towards the lower wavenumber as 1087 to 1085 (C–O), 1368 to 1326 (CH_3 bending), 1420 to 1417 (C–N), and 1667 to 1646 cm^{-1} (C═O), respectively, due to the influence of glutaraldehyde present in the crosslinked AFD. The mechanism of covalent binding of crosslinker to the amine-functionalized diatom substrates is illustrated in Scheme 1. The high-intense bands observed at 3356 cm^{-1} are due to the overlapping of amide group AFD and crosslinker (Mansur et al. 2008).

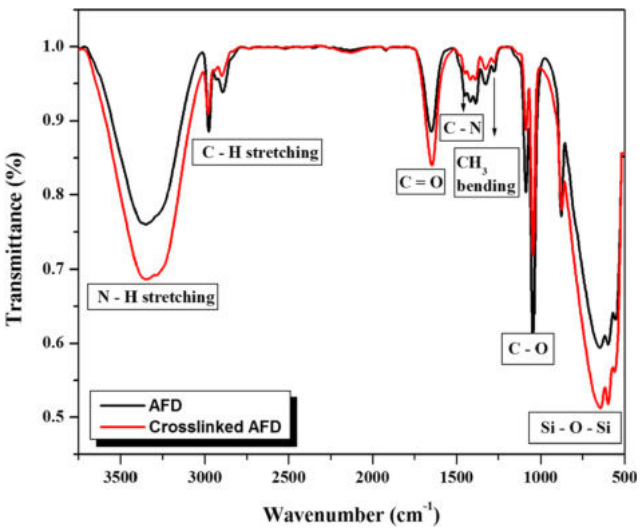

Fig. 2 FT-IR spectra of AFD and crosslinked AFD substrates

Absorption spectrum analysis

The absorption spectra of AFD and crosslinked AFD were shown in Fig. 3. The intensity of the absorption maximum gets increased compared to that of bare diatom. The optical band gap was calculated as 4.55 eV, and it was obtained by the following formula:

$$E = \frac{hC}{\lambda}$$

where, E is energy band gap, h is Plank's constant, and C is velocity of light.

This results from the blue shift of absorption maximum from 270 to 274 nm. This evidenced the influence of the crosslinker in the optical property of diatom frustules.

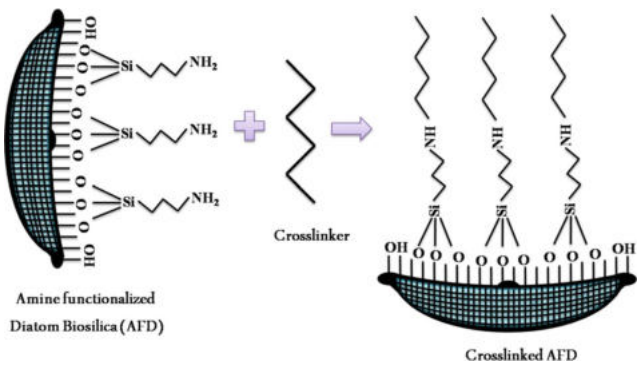

Scheme 1 Schematic diagram of attachment of crosslinker to amine-functionalized diatom substrates

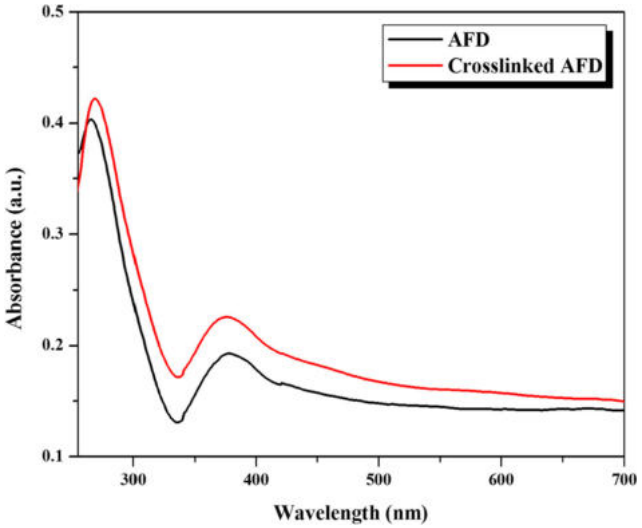

Fig. 3 UV–Vis spectra of AFD and crosslinked AFD substrates

Emission spectrum analysis

The emission spectra of AFD and crosslinked AFD were shown in Fig. 4. Due to the addition of crosslinker to the AFD, the peak intensity enhanced significantly without any peak shift. The binding efficiency of AFD was less to absorb larger antibody molecule; hence, crosslinking helps in effective binding of antibodies (Sandeep et al. 2014). The addition of glutaraldehyde (crosslinker) to AFD consequently increase its PL intensity to another one factor. The enhancement in the PL response could be attributed to the constituents of crosslinker because of its suppressed interchain interactions.

Sensing experiment

The control experiment validated the specificity of the enhanced PL emission associated with the immunocomplex of the *S. typhi* antibody-functionalized diatom frustule substrates evaluated against the *S. typhi* (complementary) and *E. coli* (non-complementary) antigens in PBS with fixed excitation wavelength which is evidenced in Figs. 5 and 6.

To know the immunospecificity of the *S. typhi* antibody-conjugated diatom frustules, *E. coli* antigen of 10^{-1} concentration was added to it. Here, there is no possible interaction or bonding formation between the *S. typhi* antibody and *E. coli* antigen because of its non-complementary nature. All the experiments were done in triplicate.

The outcomes of the above said experiment were evidenced in Fig. 7. The PL responses were obtained for the maximum concentration of *S. typhi* and *E. coli* antigens in which the *E. coli* antigen produced weak signal compared to the response of the *S. typhi* antigen. Because the biomolecules are mostly of nucleophilic moieties, when it is attached to nanomaterials or nanoscale ornate porous diatom, it can increase PL emission (Sarangi et al. 2007). According to the

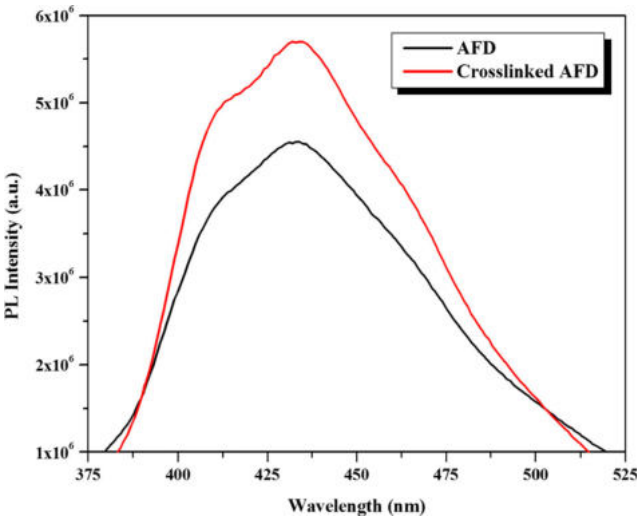

Fig. 4 PL spectra of AFD and crosslinked AFD substrates

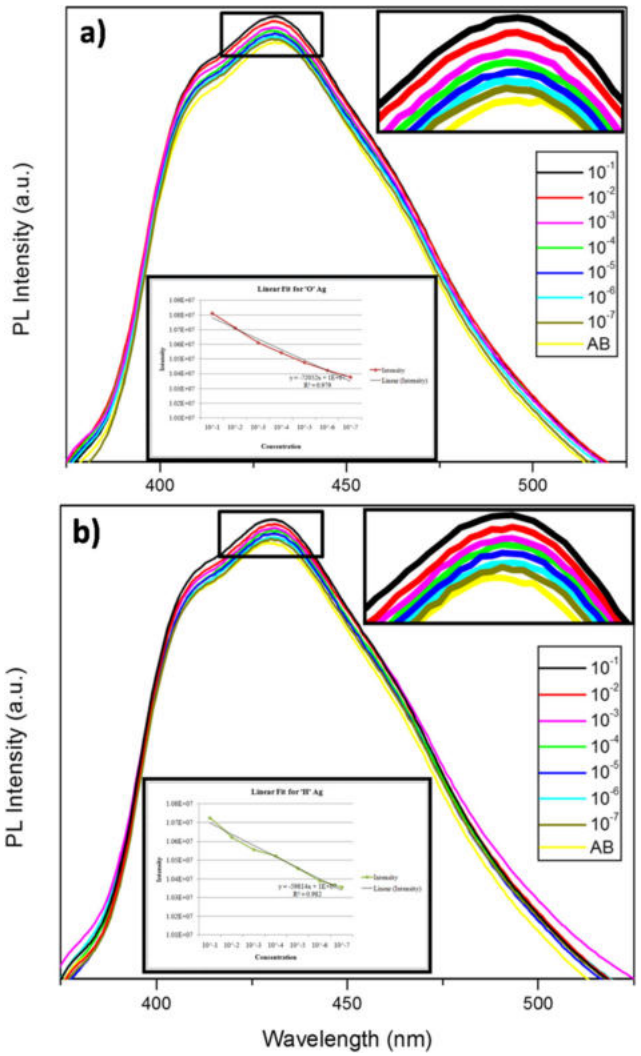

Fig. 5 PL spectra of bound (**a**) "O" antigen and (**b**) "H" antigen of *S. typhi* to the antibody-immobilized diatom substrate

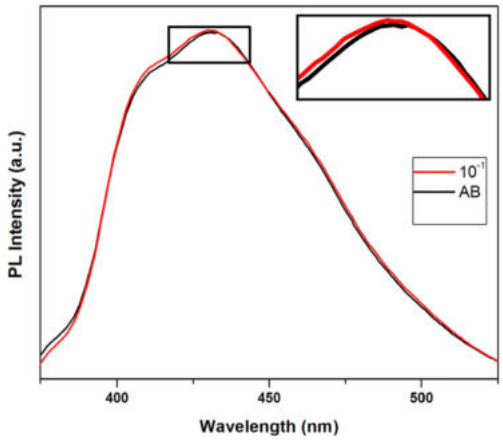

Fig. 6 PL spectra of bound *E. coli* antigen to *S. typhi* antibody-immobilized diatom substrate

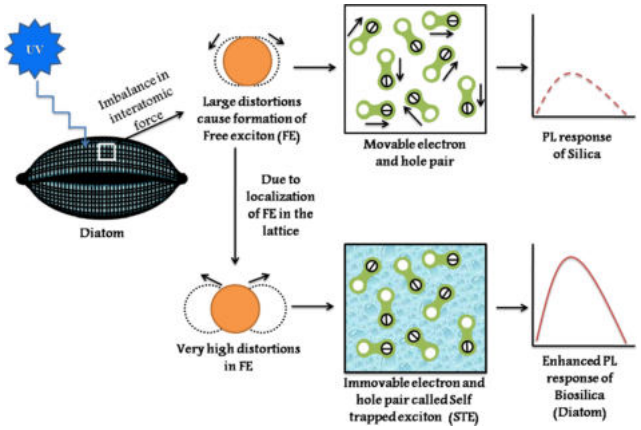

Scheme 2 Schematic diagram of photoluminescence mechanism of diatom frustules

QC/PL center model, the obtained PL responses of the diatom frustules can be compared with the properties of porous silicon. This model proposed that the quantum confinement (QC) in the silicon nanoscale is followed by de-excitation via light emitters in SiO_2-passivated layers (Qin et al. 1993). The deviation in optical and electronic properties between the bulk and nanostructured materials is resultant due to the quantum confinement effect. This model evidenced that the observed PL responses can be explained by self-trapped exciton under a quantum confinement effect in diatom frustules instead of usual band-to-band transition. The free exciton (FE) formation arises due to the sudden change of electronic charge distribution which results in imbalance among the interatomic forces. The excitonic energy reduction is caused by the self-trapping process in which the lattice of free exciton gets localized (Goswami et al. 2012). The electrons and the holes in the free exciton result in self-induced distortions in the structure, and arrest of the movement of free excitons results in self-entrapment (Scheme 2). The diatom frustules consist of porous silica, and it can be concluded that multiple peaks in PL are due to non-uniform crystallite size in the frustules. The PL intensity of 10^{-1} *S. typhi* antigen increased over 4-fold than the *S. typhi* antibody-functionalized diatom, which is because the *S. typhi* antigen is a nucleophilic molecule and when it is attached to the antibody it donates the electrons to non-radiative defect sites on the *S. typhi* antibody-functionalized diatom surface. Therefore, there is a decrease in non-radiative electron decay and increase in radiative emission which results in enhanced PL intensity after immunocomplex formation (Gale et al. 2009).

In addition, PL intensity increased only a fold than the *S. typhi* antibody-functionalized diatom when it was challenged with the 10^{-1} *E. coli* antigen, which is also a nucleophilic molecule. This is because there is no immunocomplex formation that takes place. This result demonstrated that the PL detection was selective.

From the obtained results, we can conclude that our prepared substrates can be used for the selective determination of *S. typhi* even in trace amount whereas any other non-complementary antigen may not produce relative statistical change in PL intensity.

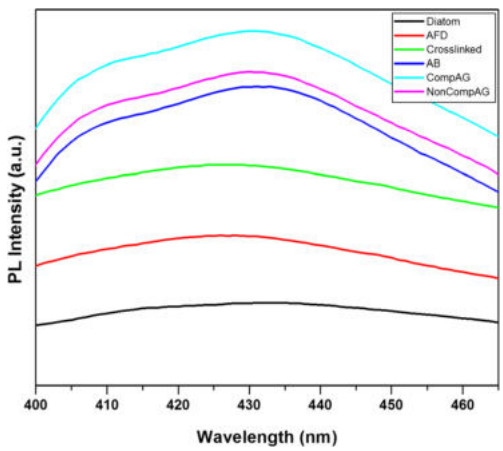

Fig. 7 Specificity of antibody-immobilized diatom substrates

Conclusion

The obtained results demonstrated that morphological feature of crosslinked diatom forms a smooth outer surface, that the presence of specific functional groups was evidenced by glutaraldehyde surface modification, that the optical band gap was calculated as 4.53 eV, and that the emission spectra illustrated an increased PL intensity by a factor of four when the complementary *S. typhi* immunocomplex is formed. It was calculated that the antibody-immobilized diatom substrates are having a detection limit of 10 pg, and hence, it can be used as a suitable sensing platform for the environment monitoring of the most serious water-borne illness, typhoid, with higher specificity.

Acknowledgements The authors thank Dr. P. Santhanam, Marine Planktonology & Aquaculture Lab, Department of Marine Science, Bharathidasan University, Tiruchirappalli, Tamilnadu, India, for providing diatom sample for this work.

Compliance with ethical standards

Conflict of interest The authors declare no potential conflicts of interest with respect to the authorship and/or publication of this article.

References

Betard A, Fischer RA (2012) Metal organic framework substrates: from fundamentals to applications. Chem Rev 112:1055–1083

De Stefano L, Rendina I, De Stefano M, Bismuto A, Maddalena P (2005) Marine diatoms as optical chemical sensors. Appl Phys Lett 87: 233902

De Stefano L, Lamberti A, Rotiroti L, De Stefano M (2008) Interfacing the nanostructured biosilica microshells of the marine diatom *Coscinodiscus wailesii* with biological matter. Acta Biomater 4: 126–130

De Stefano L, Rotiroti L, Lamberti A, Lettieri S, Setaro A, De Stefano M, Maddalena P (2009) Marine diatoms as optical biosensors. Biosens Bioelectron 24:1580–1584

Gale DK, Gutu T, Jiao J, Chang C-H, Rorrer GL (2009) Photoluminescence detection of biomolecules by antibody-functionalized diatom biosilica. Adv Funct Mater 19:926–933

Goswami B, Choudhury A, Buragohain AK (2012) Luminescence properties of a nanoporous freshwater diatom. Luminescence 27:16–19

Han D, Yan L, Chen W, Li W (2011) Preparation of chitosan/graphene oxide composite film with enhanced mechanical strength in the wet state. Carbohydr Polym 83:653–658

Lettieri S, Setaro A, De Stefano L, De Stefano M, Maddalena P (2008) The gas-detection properties of light-emitting diatoms. Adv Funct Mater 18:1257–1264

Li B, Shan C-L, Zhou Q, Fang Y, Wang Y-L, Xu F, Han L-R, Ibrahim M, Guo L-B, Xie G-L, Sun G-C (2013) Synthesis, characterization, and antibacterial activity of cross-linked chitosan-glutaraldehyde. Mar Drugs 11:1534–1552

Mansur HS, Sadahira CM, Souza AN, Mansur AAP (2008) FTIR spectroscopy characterization of poly(vinyl alcohol) hydrogel with different hydrolysis degree and chemically crosslinked with glutaraldehyde. Mater Sci Engg C 28:539–548

Pui CF, Wong WC, Chai LC, Tunung R, Jeyaletchumi P, Noor Hidayah MS, Ubong A, Farinazleen MG, Cheah YK, Son R (2011) Salmonella: a foodborne pathogen. Int Food Res J 18:465–473

Qin GG, Jia YQ (1993) Mechanism of the visible luminescence in porous silicon. Solid State Commun 86:559-563

Sandeep KV, Edmond L, Sabahudin H, Keith BM, John HTL (2014) Immobilization of antibodies and enzymes on 3-aminopropyltriethoxysilane-functionalized bioanalytical platforms for biosensors and diagnostics. Chem Rev 114:11083–11130

Sarangi SN, Goswami K, Sahu SN (2007) Biomolecular recognition in DNA tagged CdSe nanowires. Biosens Bioelectron 22:3086–3091

Sharan R, Chhibber S, Reed RH (2011) Inactivation and sub-lethal injury of *Salmonella typhi*, *Salmonella typhimurium* and *Vibrio cholerae* in copper water storage vessels. BMC Infect Dis 11:1–6

Singh A, Singh MP, Sharma V, Verma HN, Arora K (2012) Chemical analysis of food: techniques and applications. Elsevier, Amsterdam, pp 407–464

Viji S, Anbazhagi M, Ponpandian N, Mangalaraj D, Jeyanthi S, Santhanam P, Shenbaga Devi A, Viswanathan C (2014) Diatom-based label-free optical biosensor for biomolecules. Appl Biochem Biotechnol 174:1173–1166

Yu Y, Addai-Mensah J, Losic D (2010) Synthesis of self-supporting gold microstructures with three-dimensional morphologies by direct replication of diatom templates. Langmuir 26:14068–14072

Zhang XL, Jeza VT, Pan Q (2008) *Salmonella typhi*: from a human pathogen to a vaccine vector. Cell Mol Immunol 5:91–97